ELSEVIER

Contents lists available at ScienceDirect

Journal of Luminescence

journal homepage: www.elsevier.com/locate/jlumin





Carbazole-functionalized dipicolinato Ln^{III} complexes show two-photon excitation and viscosity-sensitive metal-centered emission

Jorge H.S.K. Monteiro ^{a,b,**}, Natalie R. Fetto ^{a,c}, Matthew J. Tucker ^a, Fernando A. Sigoli ^d, Ana de Bettencourt-Dias ^{a,*}

- ^a Department of Chemistry, University of Nevada, Reno, NV, 89557, United States
- ^b Department of Chemistry, Humboldt State University, Arcata, CA, 95521, United States
- ^c Department of Chemistry, Biochemistry and Physics, The University of Tampa, Tampa, FL, 33606, United States
- ^d Institute of Chemistry, University of Campinas, Campinas, São Paulo, 13083-970, Brazil

ARTICLE INFO

Keywords: Europium Ytterbium Lanthanide luminescence Two-photon absorption Two-photon absorption cross-section Viscosity sensing Carbazole-functionalized dipicolinato

ABSTRACT

Eu^{III} and Yb^{III} complexes with the carbazole-dipicolinato ligand dpaCbz²⁻, namely K_3 [Eu(dpaCbz)₃] and K_3 [Yb (dpaCbz)₃], were isolated. The Eu^{III} complex displayed metal-centered emission upon one-photon excitation with a sensitized emission efficiency Φ_{Ln}^{ID} of $1.8\pm0.3\%$, corresponding to an intrinsic emission efficiency Φ_{Ln}^{ID} of 46% and a sensitization efficiency of η_{sens} 3.9%, with an emission lifetime of the emissive state τ of 1.087 ± 0.005 ms. The Yb^{III} complex displayed Φ_{L}^{ID} of $0.010\pm0.001\%$, and a τ of 2.32 ± 0.06 µs The Eu^{III}-centered emission was sensitized as well upon two-photon excitation and a two-photon absorption cross-section σ_{2PA} of 63 GM at 750 nm was determined for the complex. The one- or two-photon sensitized emission intensity of the Eu^{III} complex changes by more than two-fold when the solvent viscosity is varied in the range 0.5-200 cP and the emission is independent of dissolved oxygen. The Yb^{III} complex displays a change in emission intensity as well. However, in this case, a dependence of the emission intensity on dissolved oxygen content was observed.

1. Introduction

The unique luminescence properties of lanthanide ($\rm Ln^{III}$) ions make them interesting as luminescent labels and in sensing applications [1–13]. The emission is based on $\it f$ - $\it f$ transitions; the latter are core orbitals and thus the transitions are line-like, leading to emission with high colour purity. Long luminescence lifetimes are observed, due to the forbidden nature of the $\it f$ - $\it f$ transitions. The long lifetimes enable time-delayed emission spectroscopy which improves signal-to-noise ratio [14–16]. However, the direct excitation is inefficient, and the antenna effect is used to sensitize the emission more efficiently through a ligand chromophore (Fig. 1a). Excitation through the antenna effect leads to a beneficial large Stokes shift of sensitized emission. In addition, use of ligand chromophores enables tuning of the chemical and spectroscopic properties of the complexes through judicious functionalization [6,14,17–20].

We reported recently a dipicolinato-based ligand functionalized with a carbazole moiety $(dpaCbz^{2-})$ to sensitize Eu^{III} and Tb^{III} emission [21]

and that the Tb^{III} complex can be used for temperature sensing due to deactivation of the $Tb^{III}\ ^5D_4$ excited state through back-energy transfer to both a triplet state and a twisted intramolecular charge transfer (TICT) [22], whose population is dependent on the viscosity of the medium [23,24]. In situ determination of viscosity is important, as it is a function of intra- and extracellular mass transport [25,26]. In addition, changes in blood and plasma viscosity can be a sign of diabetes and hypertension [25,27,28]. Finally, the properties of materials, such as hydrogels, are related to their viscosity [29,30]. While macroscopic viscosity is easily measured [25], new methods of determination are needed at the microscale, for example in the cellular environment [25], such as through the use of luminescent viscosity sensors. Molecular rotors are recent examples of such sensors [31,32]. Despite the advantages of using emissive Ln^{III} ions for imaging applications, only a few examples of viscosity sensors using these ions are known, such as Yb^{III} porphyrinato complexes with a Kläui ligand with emission lifetimes that almost tripled between 0.5 and 200 cP [33]. Some of us demonstrated sensing the viscosity using the K₃[Eu(CPAD)₃] complex, for which an increase in

^{*} Corresponding author.

^{**} Corresponding author. Department of Chemistry, University of Nevada, Reno, NV, 89557, United States. *E-mail addresses*: jorge.monteiro@humboldt.edu (J.H.S.K. Monteiro), abd@unr.edu (A. de Bettencourt-Dias).

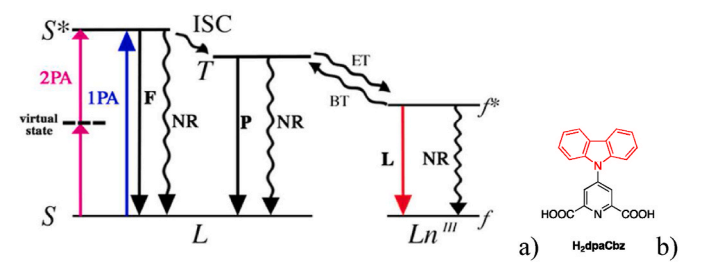


Fig. 1. a) Modified Jablønski diagram of the antenna effect with one- (1 PA) and two-photon (2 PA) absorption. F designates fluorescence, P phosphorescence, ISC intersystem crossing, ET energy transfer, BT back-transfer, L luminescence, NR non-radiative pathways, and S states with singlet and T states with triplet multiplicity [24]. b) Structure of H_2 dpaCbz (carbazole moiety highlighted in red).

the emission intensity of ~2-fold ($\lambda_{exc} = 400$ nm) or ~5.8-fold ($\lambda_{exc} = 800$ nm) in the viscosity range 0–200 cP was observed [24].

Carbazole (Fig. 1b), the functional group present in the sensitizer dpaCbz²⁻, is capable of two-photon absorption (2 PA) [34–36]. This excitation process with simultaneous absorption of two photons with half of the energy required by one-photon excitation (1 PA) (Fig. 1a) [37, 38], allows the use of excitation wavelengths in the near infrared (NIR) [39–42], the biological window in which the tissues are transparent. At these wavelengths, the quality of the images may be improved, due to deeper tissue penetration, and *in vivo* cell imaging is enabled [39,40,43, 44]. Organic dyes [45] and transition metal complexes [46] have been successfully deployed in 2 PA imaging; yet, organic dyes photobleach, and both dyes and complexes show short emission lifetimes and narrow Stokes shifts, which limits their usefulness.

The use of Ln^{III} ions, which do not suffer from these drawbacks, for 2 PA was pioneered by Lakowicz and co-workers [47,48]. Work by Maury and co-workers on dipicolinatocyclononane-based Eu^{III} complexes displaying 2 PA-sensitization showed that ligands with highly polarizable charge-transfer (CT) states result in systems with improved 2 PA cross-sections (σ_{2PA}) [38,49–52]. This work has enabled the development of Ln^{III}-based 2 PA labels dyes emitting both in the visible and NIR emitters [53-60]. In addition to labelling, Ln^{III} complexes are also useful in sensing chemical species and physicochemical properties. Palsson and co-workers demonstrated sensing of bicarbonate, a biologically relevant species in aqueous solution, using 2 PA-sensitized emission [61]. As mentioned above, our group also reported viscosity sensing, which was accomplished through 2 PA-sensitized emission [24]. Although successful, the long synthetic route to synthesize the H₂CPAD ligand and the low solubility of the complex in aqueous solution limits future applications in biological systems. To increase our knowledge of 2 PA-sensitized Ln^{III} emission and expand the number of easily accessible water-soluble LnIII-based viscosity sensors, we investigated the sensitizer dpaCbz $^{2-}$. H₂dpaCbz (Fig. 1b, Figure S1) and its Ln^{III} complexes (Ln^{III} = Eu^{III}, Gd^{III}, Yb^{III}; Figure S2) were previously isolated by the de Bettencourt-Dias and Sigoli groups [21].

2. Experimental section

All commercially obtained reagents were of analytical grade and used as received. Solvents were dried by standard methods. The stock solutions of europium(III) and ytterbium(III) chloride were prepared by dissolving the chloride salt in water. The concentration of the metal was determined by complexometric titration with EDTA (0.01 M) using xylenol orange as indicator [62].

Photophysical characterization. Solutions with concentrations 1×10^{-4} M were used to obtain the emission and excitation spectra. The photoluminescence data were obtained in a Fluorolog-3 spectrofluorimeter (Horiba FL3-22-iHR550), with an excitation monochromator

with 1200 grooves/mm and gratings blazed at 330 nm and an emission monochromator with 1200 grooves/mm and gratings blazed at 500 nm. An ozone-free 450 W xenon lamp (Ushio) was used as radiation source. The excitation spectra, corrected for instrumental function, were measured between 250 and 500 nm. The emission spectra were measured in the range 550-725 nm using a Hamamatsu 928P detector. All emission spectra were corrected for instrumental function. The emission decay curves were obtained using a TCSPC system and a Xe pulsed lamp as excitation source, for the EuIII complex, or a Horiba SpectraLED model S-370 (peak wavelength = 370 \pm 10 nm, \sim 4 pJ/ pulse), for the Yb^{III} complex. The energies of the ligand's singlet and triplet levels were obtained at ~77 K by deconvolution of the fluorescence and phosphorescence spectra, respectively, into their Franck-Condon progression and are reported as the 0-0 transition [63]. The quantum yield of the sensitized emission (ϕ_I^{Eu}) of the Eu^{III} complex was determined using an integrating sphere (model F-3018) coupled directly to the spectrofluorimeter. A solution containing only the solvent was used as blank, and then was replaced by a solution containing the compound. The sample was measured on- and -out-of-the beam path in order to account for any re-absorption effects. The quantum yield of the samples, as percentage, was determined using Equation (1).

$$\Phi = \frac{(I_B - I_S)}{(L_S - L_B)} \times 100 \tag{1}$$

L and I are the scattering and emission integrated areas, respectively. The subscripts B and S stand for blank and sample, respectively.

For the Yb^{III} complex the quantum yield was determined by the dilution method using Equation (2). The standard for quantum yield measurements was [Yb(tta)₃(H₂O)₂] ($\phi \sim 0.12$, in air-saturated toluene) [64]. The excitation wavelength for sample and quantum yield standard was chosen to ensure a linear relationship between the intensity of emitted light and the concentration of the absorbing/emitting species (A < 0.05).

$$\Phi_{x} = \frac{Grad_{x}}{Grad_{std}} \times \frac{n_{x}^{2}}{n_{x-d}^{2}} \times \frac{I_{std}}{I_{x}} \Phi_{std}$$
(2)

Grad is the slope of the plot of the emission area as a function of absorbance, n is the refractive index of the solvent, I is the intensity of the excitation source at the excitation wavelength and Φ is the quantum yield for sample x and standard std.

The intrinsic quantum yield ϕ_{Eu}^{Eu} was determined using equation (3).

$$\phi_{Eu}^{Eu} = \frac{A_{rad}}{A_{tot}} \tag{3}$$

 A_{tot} is the total emission rate ($A_{tot} = k_R + k_{NR} = 1/\tau_{exp}$) and A_{rad} is the radiative emission rate [65].

The sensitization efficiency (η_{sens}) was determined using equation (4).

$$\eta_{sens} = \frac{\phi_L^{Eu}}{\phi_L^{Eu}} \tag{4}$$

Two-photon emission setup. A Spectraphysics Mai Tai Ti:Sapphire tunable laser generates 80 fs excitation pulses centered between 710 and 820 nm. This excitation pulse propagates toward a pair of chirped mirrors (Femtolasers GSM216), introduced to compensate for any dispersion introduced from other optics. A half wave plate (Thorlabs WPH10M - 780) was placed in the beam path and set at the magic angle 54.7° to remove polarization dependence. In order to modulate the power, a neutral density filter was utilized with an OD varying between 0.4 and 0.8. The incident pulse was focused using a 100 mm convex lens (Thorlabs LA1509) into the center of a 1 cm quartz sample cell. The emission of the sample was collected at a right angle by a reflective objective (20× magnification) and focused into an Ocean Optics USB2000+ UV-VIS Spectrometer. The typical spectral range used on the spectrometer was 180 nm–870 nm. The excitation wavelengths of 720

Table 1
Photophysical data of the dpaCbz²⁻ complexes of Eu^{III} and Tb^{III}. *S* and *T* denote the singlet and triplet state energies of the ligand, respectively, τ the emission lifetime, Φ_{Ln}^{In} the intrinsic emission efficiency, Φ_{L}^{In} the sensitized emission efficiency, η_{sens} the sensitization efficiency, and σ_{2PA} the two-photon absorption cross-section. $\lambda_{exc} = 340$ nm.

| Complex | Solvent ^a | S^{b} [cm ⁻¹] | T ^b [cm ⁻¹] | τ | ϕ_{Ln}^{Ln} [%] | ϕ_L^{Ln} [%] | η _{sens} [%] | $\sigma_{\mathrm{2PA}}^{\mathrm{c}} [\mathrm{GM}]^{\mathrm{d}}$ |
|---|----------------------|--------------------------------------|------------------------------------|-----------------------|----------------------|---------------------|-----------------------|--|
| K ₃ [Eu(dpaCbz) ₃] | Water:DMSO | 26,030±400 [21] | 23,460±350 [21] | 1.087±0.005 ms | 46 | 1.8±0.3 | 3.9 | 63±8 |
| $K_3[Yb(dpaCbz)_3]$ | Water:DMSO | | | $2.32{\pm}0.06~\mu s$ | - | $0.010 {\pm} 0.001$ | _ | _ |

- ^a In aqueous TRIS/HCl buffered solution (pH \sim 7.4, 4% DMSO).
- ^b As the Gd^{III} complex at 77 K [63].
- ^c $\lambda_{exc} = 750$ nm.
- $^{\rm d}$ 1 GM = 10^{-50} cm⁴ s photon⁻¹ molecule⁻¹.

nm and 750 nm were chosen for linearity of signal with sample concentration as well as to enable direct comparison of the $\mathrm{Eu}^{\mathrm{III}}$ complex with the 2 PA rhodamine B standard.

Two-photon absorption cross section. The two photon absorption cross sections were determined via a Two-Photon Excited Fluorescence (TPEF) procedure using equation (5) [52].

$$\sigma_{2PA} = \frac{F}{F_r} \frac{\phi^r}{\phi} \frac{c^r}{c} \sigma^r_{2PA},\tag{5}$$

F are the fluorescence intensities, ϕ are the luminescence quantum yields, c are the concentrations, and the superscript r denotes the reference compound. For the Eu^{III} complexes $\phi = \phi_L^{Eu}$. Rhodamine B in methanol was used as the reference at 750 nm with $\phi^r = 70\%$ and $\sigma_{2PA}^r = 67$ GM [66]. The concentration of the reference varied between 0.1 and 1 mM. The cross section of K₃[Eu(dpaCbz)₃] (0.2 mM) in TRIS/HCl aqueous solution (pH \sim 7.4, 4% DMSO) was determined by exciting the sample at 750 nm followed by collecting the spectra using an integration time of 10 s, a boxcar width of 2 pixels, and a power ranging from 200 to 270 mW. The intensity for all samples was determined by integrating the spectrum from 550 nm to 715 nm.

Emission Intensity Dependence. The laser power was varied between 50 and 420 mW to determine the effect of the laser power on the intensity of the spectrum at 615 nm. The power dependence of the two-photon excited emission of $K_3[Eu(dpaCbz)_3]$ was determined at an excitation wavelength of 750 nm. Similar collection parameters were utilized as described above for the two-photon cross section measurements. All spectra were found to have a linear relationship between the log of the intensity and the log of the power at the λ_{max} .

Excitation Scans. The intensity at 615 nm was determined upon excitation between 710 and 820 nm. Similar collection parameters were used as described above.

Viscosity Sensing Measurements. 0.2 mM solutions of K_3 [Eu (dpaCbz)₃] were prepared in different mixtures of methanol and glycerol to obtain a wide range of viscosities. The emission spectra were obtained exciting at 336 nm, for one-photon absorption, or at 720 nm, for two-photon excitation, and P=235 mW. The intensity of the $^5D_0 \rightarrow ^7F_2$ transition was plotted as a function of the viscosity.

3. Results and discussion

As in other solvents [21,22], upon excitation at 340 nm, $K_3[Ln\ (dpaCbz)_3]\ (Ln=Eu^{III}\ and\ Yb^{III})\ in\ TRIS/HCl\ buffered\ water:DMSO\ display the characteristic Eu^{III}-centered <math>^5D_0\rightarrow^7F_J\ (J=0-4)$ (Figure S3a right) and characteristic Yb^{III}-centered $^2F_{5/2}\rightarrow ^2F_{7/2}$ emissions (Figure S3b right). The excitation spectra (Figures S3a and S3b left) resemble the absorption spectrum of the ligand [22], as expected for sensitized emission. The efficiencies of sensitization of 3.9% and of sensitized emission of 1.8% (Table 1) for the Eu^{III} emission are moderate, despite the favorable triplet state energy, intrinsic emission efficiency and emission lifetime. The moderate values are attributed to the long donor-acceptor distance of 6.5146 Å that decreases the energy transfer probability [21]. For Yb^{III}, the efficiency of sensitized emission is 0.10% and comparable to other Yb^{III}-dipicolinato complexes, as is the

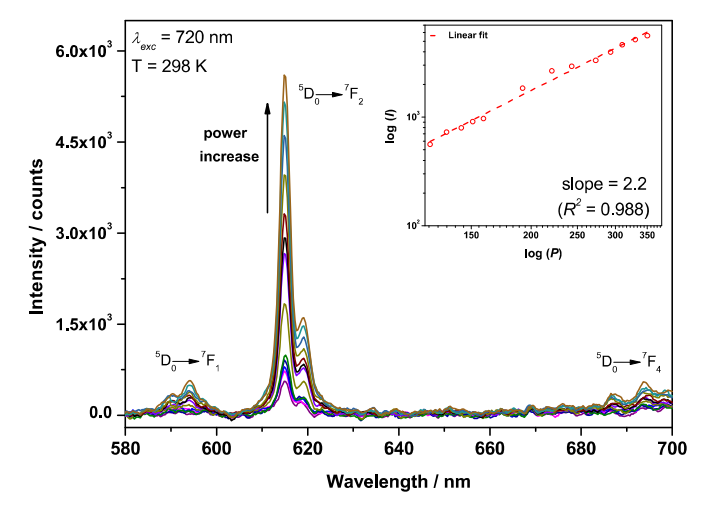


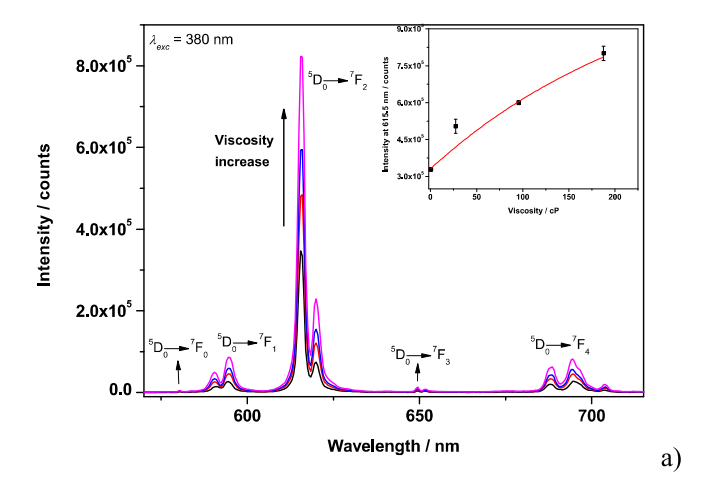
Fig. 2. Emission spectra of the complex $K_3[Eu(dpaCbz)_3]$ obtained at different laser powers. The inset shows the plot of log (I) as a function of log (P). [complex] = 0.2 mM in TRIS/HCl buffered solution (4% DMSO, pH \sim 7.4).

excited state lifetime of 2.32 μ s (Table 1) [50,67–70].

2 PA excitation of the Eu^{III} complex is accomplished in a broad range of wavelengths, as shown in Figure S4; for our studies we excited the complex at 720 or 750 nm to enable comparison with the 2 PA standard rhodamine B (Figure S5) [66]. Upon 2 PA, the characteristic metal-centered emission pattern is observed (Fig. 2). The emission intensity I shows a quadratic dependence on the laser power P (Inset of Fig. 2), which confirms the 2 PA process. The 1 PA and 2 PA emission spectra are identical (Figures 2 and S3a), as expected for processes which involve the same excited state.

At 63 GM, the σ_{2PA} for the Eu^{III} complex (Table 1) is an order of magnitude lower than for known Eu^{III} complexes [24,50]. Yet this ligand, which can be easily synthesized in one step, as opposed to other known complexes, is very versatile, as it displays 2 PA to sensitize Eu^{III} emission and its Tb^{III} complex can be used for temperature sensing [22].

The presence of a twisted intramolecular charge-transfer (TICT) state in dpaCbz²⁻, across the carbazole and pyridine functional groups [22, 23], was confirmed through the temperature dependence of the phosphorescence spectra of the analogous Gd^{III} complex, that displayed maxima at 500 and 440 nm at 298 and 77 K, respectively [22]. As changes in viscosity lead changes in population of CT states [23], we prepared solutions of $K_3[Ln(dpaCbz)_3]$ ($Ln = Eu^{III}$ or Yb^{III}) in varying ratios of methanol and glycerol to isolate solutions with viscosities in the range 0.5–200 cP. The $K_3[Eu(dpaCbz)_3]$ complex shows a more than doubling of its emission intensity under both one- and two-photon excitation (Fig. 3a and b), a similar increase to the two other known Ln^{III} -based viscosity sensors [24,33]. Thus, this complex is the second reported viscosity sensor using two-photon sensitized Eu^{III} -centered emission. An increase in emission intensity as a function of the viscosity was observed for the Yb^{III} complex as well (Figure S6a). However, this



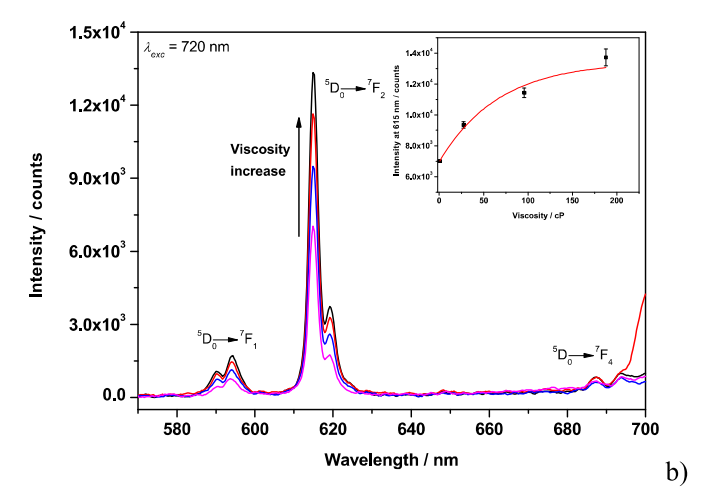


Fig. 3. (a) Emission spectra of $K_3[Eu(dpaCbz)_3]$ ($\lambda_{exc}=380$ nm) upon one-photon excitation with varying viscosities. (b) Emission spectra of $K_3[Eu(dpaCbz)_3]$ ($\lambda_{exc}=720$ nm) upon two-photon excitation with varying viscosities. The insets show the plot of the emission intensity at 615 nm as a function of viscosity. [complex] = 0.2 mM. Solutions with varying ratios of MeOH: glycerol were used with viscosity in the range 0.5–200 cP.

intensity change was strongly dependent upon O_2 concentration (Figure S6b), consistent with non-radiative quenching of the ligand's triplet level though interaction with oxygen, which in turn decreases the metal ion's emission lifetime [71], indicating that in this complex this pathway is competitive with the energy transfer from the triplet level to the emissive state of Yb^{III}. Thus, the use of this Yb^{III} complex for viscosity sensing will not be further discussed. Nonetheless, while not pursued here, this oxygen sensitivity makes the complex interesting as an oxygen sensor.

Methanol and glycerol have different amounts of dissolved oxygen; the mole fractions at 298 K and 101.3 kPa are 4.15×10^{-4} for methanol and 4.8×10^{-6} – 5.5×10^{-6} for glycerol [72,73]. To ensure that emission behavior in the case of the Eu^{III} complex is due to solvent viscosity, and not quenching through oxygen [71,74], the emission lifetimes were determined. At 1.497 ± 0.002 ms in methanol, and 1.604 ± 0.006 ms in 1:9 methanol:glycerol (Figures S7 – S10), these are non-equivalent, confirming quenching of the triplet level of the ligand by molecular O_2 . To determine the extent of the O_2 influence, we investigated the emission intensity of the 0.2 mM solutions of $K_3[Eu(dpaCbz)_3]$ with varying amounts of methanol and glycerol in the absence of O_2 . Although the concentration of O_2 slightly influences the emission intensity of $K_3[Eu(dpaCbz)_3]$ in pure methanol, it does not influence it in other methanol:glycerol solvent mixtures (Figure S11). That indicates that a high concentration of O_2 is needed to have a significant effect, and

Table 2 Emission lifetimes of $K_3[Eu(dpaCbz)_3]$ in the presence (τ_{O2}) and absence $(\tau_{no\ O2})$ of oxygen.

| Solvent | τ_{O2}^{a} [ms] | $\tau_{no~O2}^{b}$ [ms] |
|-----------------------|----------------------|-------------------------|
| Methanol | $1.497{\pm}0.002$ | 1.599 ± 0.003 |
| 1:9 methanol:glycerol | $1.604{\pm}0.006$ | 1.604 ± 0.003 |

[complex] = 0.2 mM, λ_{exc} = 380 nm.

- Determined in the presence of O₂.
- b Determined in the absence of O₂.

the observed emission intensity changes are almost exclusively due to viscosity changes. The emission lifetimes of the $K_3[Eu(dpaCbz)_3]$ complex in degassed methanol and degassed 1:9 methanol:glycerol are equivalent, which further confirms that the emission intensity changes are due to viscosity changes (Table 2 and Figures S7 – S10).

Another solvent property, namely its polarity, can influence the emission intensity of the Ln^{III} as well, as high polarity solvents can stabilize ligand CT states [75] and thus the excited state energy of the ligand, which changes the ligand \rightarrow Ln^{III} energy transfer rates. To ensure that the energy of the ligand excited state is not affected by the solvent polarity, the phosphorescence spectra of the [Gd(dpaCbz)₃] complex were obtained in 100% methanol and 1:9 methanol:glycerol (Figure S12). The lack of significant change of the phosphorescence emission bands confirms that the emission intensity changes are solely due to the viscosity of the medium.

4. Conclusions

In summary, Ln^{III} complexes with an easily synthesized carbazole-functionalized pyridine-bis(carboxylate) chelator display Eu^{III} and Yb^{III} emission. Eu^{III} emission using two-photon absorption was observed with a σ_{2PA} of 63 GM. A change in emission intensity as a function of the viscosity was observed for the Eu^{III} complex upon excitation with one-photon and, as a rare example, using two-photon excitation. These results establish this carbazole-based ligand as a versatile building block in temperature and viscosity sensing and in 2 PA dyes. These results contribute to our knowledge in the fields of imaging, sensing of physicochemical properties in materials and diagnosis in microscale systems.

Author statement

Jorge H. S. K. Monteiro conceptualized and did most of the work, including manuscript draft. Natalie R. Fetto performed two-photon measurements in collaboration with JHSKM. Matthew J. Tucker supervised the two-photon measurements and procured funding. Fernando A. Sigoli conceptualized the project. Ana de Bettencourt-Dias conceptualized the project, procured funding and supervised the entirety of the project.

Declaration of competing interest

The authors declare that they have no known competing financial interests or personal relationships that could have appeared to influence the work reported in this paper.

Acknowledgments

Financial support from NSF-CHE 1800392 (AdBD), NIH R15GM1224597 (MJT), and FAPESP 2013/22127-2 and 2014/50906-9 (FAS) is gratefully acknowledged.

Appendix A. Supplementary data

Supplementary data to this article can be found online at https://doi.org/10.1016/j.jlumin.2022.118768.

References

- [1] J.-C.G. Bünzli, Lanthanide luminescence for biomedical analyses and imaging, Chem. Rev. 110 (2010) 2729–2755.
- [2] J. Zhao, J. Gao, W. Xue, Z. Di, H. Xing, Y. Lu, L. Li, Upconversion luminescenceactivated DNA nanodevice for ATP sensing in living cells, J. Am. Chem. Soc. 140 (2018) 578–581.
- [3] J. Hai, T. Li, J. Su, W. Liu, Y. Ju, B. Wang, Y. Hou, Anions reversibly responsive luminescent Tb(III) nanocellulose complex hydrogels for latent fingerprint detection and encryption, Angew. Chem. Int. Ed. 57 (2018) 6786–6790.
- [4] M. Cardoso Dos Santos, A. Runser, H. Bartenlian, A.M. Nonat, L.J. Charbonnière, A. S. Klymchenko, N. Hildebrandt, A. Reisch, Lanthanide-complex-loaded polymer nanoparticles for background-free single-particle and live-cell imaging, Chem. Mater. 31 (2019) 4034–4041.
- [5] R. Arppe-Tabbara, M.R. Carro-Temboury, C. Hempel, T. Vosch, T.J. Sorensen, Luminescence from lanthanide(III) ions bound to the glycocalyx of Chinese hamster ovary cells, Chem. Eur J. 24 (2018) 11885–11889.
- [6] J. Monteiro, D. Machado, L.M. de Hollanda, M. Lancellotti, F.A. Sigoli, A. de Bettencourt-Dias, Selective cytotoxicity and luminescence imaging of cancer cells with a dipicolinato-based Eu-III complex, Chem. Commun. 53 (2017) 11818–11821.
- [7] Y. Ning, S. Chen, H. Chen, J.-X. Wang, S. He, Y.-W. Liu, Z. Cheng, J.-L. Zhang, A proof-of-concept application of water-soluble ytterbium(iii) molecular probes in in vivo NIR-II whole body bioimaging, Inorg. Chem. Front. 6 (2019) 1962–1967.
- [8] Y. Ning, S. Cheng, J.-X. Wang, Y.-W. Liu, W. Feng, F. Li, J.-L. Zhang, Fluorescence lifetime imaging of upper gastrointestinal pH in vivo with a lanthanide based nearinfrared τ probe, Chem. Sci. 10 (2019) 4227–4235.
- [9] Y. Ning, J. Tang, Y.-W. Liu, J. Jing, Y. Sun, J.-L. Zhang, Highly luminescent, biocompatible ytterbium(iii) complexes as near-infrared fluorophores for living cell imaging, Chem. Sci. 9 (2018) 3742–3753.
- [10] H. Li, C. Xie, R. Lan, S. Zha, C.-F. Chan, W.-Y. Wong, K.-L. Ho, B.D. Chan, Y. Luo, J.-X. Zhang, G.-L. Law, W.C.S. Tai, J.-C.G. Bünzli, K.-L. Wong, A smart europium-ruthenium complex as anticancer prodrug: controllable drug release and real-time monitoring under different light excitations, J. Med. Chem. 60 (2017) 8923–8932.
- [11] D. Li, S. He, Y. Wu, J. Liu, Q. Liu, B. Chang, Q. Zhang, Z. Xiang, Y. Yuan, C. Jian, A. Yu, Z. Cheng, Excretable lanthanide nanoparticle for biomedical imaging and surgical navigation in the second near-infrared window, Adv. Sci. 6 (2019), 1902042-1902042.
- [12] L. Yang, K. Zhang, S. Bi, J.-J. Zhu, Dual-acceptor-based upconversion luminescence nanosensor with enhanced quenching efficiency for in situ imaging and quantification of MicroRNA in living cells, ACS Appl. Mater. Interfaces 11 (2019) 38459–38466.
- [13] T. Liang, Z. Li, P. Wang, F. Zhao, J. Liu, Z. Liu, Breaking through the signal-to-background limit of upconversion nanoprobes using a target-modulated sensitizing switch, J. Am. Chem. Soc. 140 (2018) 14696–14703.
- [14] J.-C.G. Bünzli, On the design of highly luminescent lanthanide complexes, Coord. Chem. Rev. 293–294 (2015) 19–47.
- [15] A. de Bettencourt-Dias, Introduction to lanthanide ion luminescence, in: A. de Bettencourt-Dias (Ed.), Luminescence of Lanthanide Ions in Coordination Compounds and Nanomaterials, Wiley, 2014.
- [16] J.-C.G. Bünzli, C. Piguet, Taking advantage of luminescent lanthanide ions, Chem. Soc. Rev. 34 (2005) 1048–1077.
- [17] G.L. Law, R. Pal, L.O. Palsson, D. Parker, K.L. Wong, Responsive and reactive terbium complexes with an azaxanthone sensitiser and one naphthyl group: applications in ratiometric oxygen sensing in vitro and in regioselective cell killing, Chem. Commun. (2009) 7321–7323, 0.
- [18] J.-C.G. Bünzli, S.V. Eliseeva, Basics of lanthanide photophysics, in: P. Hänninen, H. Härmä (Eds.), Lanthanide Luminescence: Photophysical, Analytical and Biological Aspects, Springer, Berlin, 2011, pp. 1–46.
- [19] E. Pershagen, J. Nordholm, K.E. Borbas, Luminescent lanthanide complexes with analyte-triggered antenna formation, J. Am. Chem. Soc. 134 (2012) 9832–9835.
- [20] C. Szijjarto, E. Pershagen, N.O. Ilchenko, K.E. Borbas, A versatile long-wavelengthabsorbing scaffold for Eu-based responsive probes, Chemistry 19 (2013) 3099–3109.
- [21] J.H.S.K. Monteiro, A. de Bettencourt-Dias, F.A. Sigoli, Estimating the donor–acceptor distance to tune the emission efficiency of luminescent lanthanide compounds, Inorg. Chem. 56 (2017) 709–712.
- [22] J.H.S.K. Monteiro, F.A. Sigoli, A. de Bettencourt-Dias, A water-soluble TbIII complex as a temperature-sensitive luminescent probe, Can. J. Chem. (2017) 1–6.
- [23] S. Sasaki, G.P.C. Drummen, G. Konishi, Recent advances in twisted intramolecular charge transfer (TICT) fluorescence and related phenomena in materials chemistry, J. Mater. Chem. C 4 (2016) 2731–2743.
- [24] J.H.S.K. Monteiro, N.R. Fetto, M.J. Tucker, A. de Bettencourt-Dias, Luminescent carbazole-based EuIII and YbIII complexes with a high two-photon absorption cross-section enable viscosity sensing in the visible and near IR with one- and twophoton excitation, Inorg. Chem. 59 (2020) 3193–3199.
- [25] Z. Yang, J. Cao, Y. He, J.H. Yang, T. Kim, X. Peng, J.S. Kim, Macro-/micro-environment-sensitive chemosensing and biological imaging, Chem. Soc. Rev. 43 (2014) 4563–4601.
- [26] M.K. Kuimova, S.W. Botchway, A.W. Parker, M. Balaz, H.A. Collins, H.L. Anderson, K. Suhling, P.R. Ogilby, Imaging intracellular viscosity of a single cell during photoinduced cell death, Nat. Chem. 1 (2009) 69–73.
- [27] M.K. Kuimova, Mapping viscosity in cells using molecular rotors, Phys. Chem. Chem. Phys. 14 (2012) 12671–12686.

- [28] G. Sloop, R.E. Holsworth, J.J. Weidman, J.A. St Cyr, The role of chronic hyperviscosity in vascular disease, Therap. Adv. Cardiovascular Disease 9 (2014) 10, 25
- [29] M.H. Chen, L.L. Wang, J.J. Chung, Y.-H. Kim, P. Atluri, J.A. Burdick, Methods to assess shear-thinning hydrogels as injectable biomaterials, ACS Biomater. Sci. Eng. 3 (2017) 3146–3160.
- [30] E.A. Corbin, L.J. Millet, J.H. Pikul, C.L. Johson, J.G. Georgiadis, W.P. King, R. Bashir, Micromechanical properties of hydroegls measured with MEMS resonant sensors, in: M. Ferrari (Ed.), Biomedical Microdevices, Springer, 2012.
- [31] M.A. Haidekker, T.P. Brady, D. Lichlyter, E.A. Theodorakis, A ratiometric fluorescent viscosity sensor, J. Am. Chem. Soc. 128 (2006) 398–399.
- [32] M.K. Kuimova, G. Yahioglu, J.A. Levitt, K. Suhling, Molecular rotor measures viscosity of live cells via fluorescence lifetime imaging, J. Am. Chem. Soc. 130 (2008) 6672. +.
- [33] Y. Ning, Y.-W. Liu, Y.-S. Meng, J.-L. Zhang, Design of near-infrared luminescent lanthanide complexes sensitive to environmental stimulus through rationally tuning the secondary coordination sphere, Inorg. Chem. 57 (2018) 1332–1341.
- [34] M. Lepeltier, F. Appaix, Y.Y. Liao, F. Dumur, J. Marrot, T. Le Bahers, C. Andraud, C. Monnereau, Carbazole-substituted iridium complex as a solid state emitter for two-photon intravital imaging, Inorg. Chem. 55 (2016) 9586–9595.
- [35] X.L. Hao, L. Zhang, D. Wang, C. Zhang, J.F. Guo, A.M. Ren, Analyzing the effect of substituents on the photophysical properties of carbazole-based two-photon fluorescent probes for hypochlorite in mitochondria, J. Phys. Chem. C 122 (2018) 6273–6287.
- [36] P.Z. Chen, J.X. Wang, L.Y. Niu, Y.Z. Chen, Q.Z. Yang, Carbazole-containing difluoroboron beta-diketonate dyes: two-photon excited fluorescence in solution and grinding-induced blue-shifted emission in the solid state, J. Mater. Chem. C 5 (2017) 12538–12546.
- [37] F. Terenziani, C. Katan, E. Badaeva, S. Tretiak, M. Blanchard-Desce, Enhanced two-photon absorption of organic chromophores: theoretical and experimental assessments, Adv. Mater. 20 (2008) 4641–4678.
- [38] C. Andraud, O. Maury, Lanthanide complexes for nonlinear optics: from fundamental aspects to applications, Eur. J. Inorg. Chem. (2009) 4357–4371, 2009.
- [39] T. Ren, W. Xu, Q. Zhang, X. Zhang, S. Wen, H. Yi, L. Yuan, X. Zhang, Harvesting hydrogen bond network: enhance the anti-solvatochromic two-photon fluorescence for cirrhosis imaging, Angew. Chem. Int. Ed. 57 (2018) 7473–7477.
- [40] B.K. Agrawalla, H.W. Lee, W.H. Phue, A. Raju, J.J. Kim, H.M. Kim, N.Y. Kang, Y. T. Chang, Two-photon dye cocktail for dual-color 3D imaging of pancreatic beta and alpha cells in live islets, J. Am. Chem. Soc. 139 (2017) 3480–3487.
- [41] W. Denk, J.H. Strickler, W.W. Webb, 2-PHOTON laser scanning fluorescence microscopy, Science 248 (1990) 73–76.
- [42] F. Helmchen, W. Denk, Deep tissue two-photon microscopy, Nat. Methods 2 (2005)
- [43] B.K. Agrawalla, Y. Chandran, W.H. Phue, S.C. Lee, Y.M. Jeong, S.Y.D. Wan, N. Y. Kang, Y.T. Chang, Glucagon-secreting alpha cell selective two-photon fluorescent probe TP-alpha: for live pancreatic islet imaging, J. Am. Chem. Soc. 137 (2015) 5355–5362.
- [44] P. Kumari, S.K. Verma, S.M. Mobin, Water soluble two-photon fluorescent organic probes for long-term imaging of lysosomes in live cells and tumor spheroids, Chem. Commun. 54 (2018) 539–542.
- [45] B. Li, L. Lu, M. Zhao, Z. Lei, F. Zhang, An efficient 1064 nm NIR-II excitation fluorescent molecular dye for deep-tissue high-resolution dynamic bioimaging, Angew. Chem. Int. Ed. 57 (2018) 7483–7487.
- [46] J.S. Nam, M.G. Kang, J. Kang, S.Y. Park, S.J.C. Lee, H.T. Kim, J.K. Seo, O.H. Kwon, M.H. Lim, H.W. Rhee, T.H. Kwon, Endoplasmic reticulum-localized iridium(III) complexes as efficient photodynamic therapy agents via protein modifications, J. Am. Chem. Soc. 138 (2016) 10968–10977.
- [47] J.R. Lakowicz, G. Piszczek, B.P. Maliwal, I. Gryczynski, Multiphoton excitation of lanthanides, ChemPhysChem: Eur.J. Chem. Phys. Phys. Chem. 2 (2001) 247–252.
- [48] G. Piszczek, B.P. Maliwal, I. Gryczynski, J. Dattelbaum, J.R. Lakowicz, Multiphoton ligand-enhanced excitation of lanthanides, J. Fluoresc. 11 (2001) 101–107.
- [49] A. D'Aléo, F. Pointillart, L. Ouahab, C. Andraud, O. Maury, Charge transfer excited states sensitization of lanthanide emitting from the visible to the near-infra-red, Coord. Chem. Rev. 256 (2012) 1604–1620.
- [50] A. D'Aleo, A. Picot, P.L. Baldeck, C. Andraud, O. Maury, Design of dipicolinic acid ligands for the two-photon sensitized luminescence of europium complexes with optimized cross-sections, Inorg. Chem. 47 (2008) 10269–10279.
- [51] A. Picot, F. Malvolti, B. Le Guennic, P.L. Baldeck, J.A.G. Williams, C. Andraud, O. Maury, Two-photon antenna effect induced in octupolar europium complexes, Inorg. Chem. 46 (2007) 2659–2665.
- [52] A. D'Aléo, C. Andraud, O. Maury, Two-photon absorption of lanthanide complexes: from fundamental aspects to biphotonic imaging applications, in: Luminescence of Lanthanide Ions in Coordination Compounds and Nanomaterials, John Wiley & Sons Ltd, Chichester, 2014, pp. 197–230.
- [53] A. Picot, A. D'Aleo, P.L. Baldeck, A. Grichine, A. Duperray, C. Andraud, O. Maury, Long-lived two-photon excited luminescence of water-soluble europium complex: applications in biological imaging using two-photon scanning microscopy, J. Am. Chem. Soc. 130 (2008) 1532–1533.
- [54] A. Grichine, A. Haefele, S. Pascal, A. Duperray, R. Michel, C. Andraud, O. Maury, Millisecond lifetime imaging with a europium complex using a commercial confocal microscope under one or two-photon excitation, Chem. Sci. 5 (2014) 3475–3485.
- [55] A.T. Bui, A. Grichine, S. Brasselet, A. Duperray, C. Andraud, O. Maury, Unexpected efficiency of a luminescent samarium(III) complex for combined visible and nearinfrared biphotonic microscopy, Chem. Eur J. 21 (2015) 17757–17761.

- [56] G.L. Law, K.L. Wong, C.W.Y. Man, S.W. Tsao, W.T. Wong, A two-photon europium complex as specific endoplasmic reticulum probe, J. Biophot. 2 (2009) 718–724.
- [57] V. Placide, A.T. Bui, A. Grichine, A. Duperray, D. Pitrat, C. Andraud, O. Maury, Two-photon multiplexing bio-imaging using a combination of Eu- and Tbbioprobes, Dalton Trans. 44 (2015) 4918–4924.
- [58] A.T. Bui, M. Beyler, Y.Y. Liao, A. Grichine, A. Duperray, J.C. Mulatier, B. Le Guennic, C. Andraud, O. Maury, R. Tripier, Cationic two-photon lanthanide bioprobes able to accumulate in live cells, Inorg. Chem. 55 (2016) 7020–7025.
- [59] N. Hamon, M. Galland, M. Le Fur, A. Roux, A. Duperray, A. Grichine, C. Andraud, B. Le Guennic, M. Beyler, O. Maury, R. Tripier, Combining a pyclen framework with conjugated antenna for the design of europium and samarium luminescent bioprobes, Chem. Commun. 54 (2018) 6173–6176.
- [60] N. Hamon, A. Roux, M. Beyler, J.-C. Mulatier, C. Andraud, C. Nguyen, M. Maynadier, N. Bettache, A. Duperray, A. Grichine, S. Brasselet, M. Gary-Bobo, O. Maury, R. Tripier, Pyclen-based In(III) complexes as highly luminescent bioprobes for in vitro and in vivo one- and two-photon bioimaging applications, J. Am. Chem. Soc. 142 (2020) 10184–10197.
- [61] L.O. Palsson, R. Pal, B.S. Murray, D. Parker, A. Beeby, Two-photon absorption and photoluminescence of europium based emissive probes for bioactive systems, Dalton Trans. (2007) 5726–5734, 0.
- [62] J. Bassett, R.C. Denney, G.H. Jeffery, J. Mendham, Vogel's Textbook of Quantitative Inorganic Analysis, fourth ed. ed., Longman Group, London, 1978.
- [63] G.A. Crosby, R.E. Whan, R.M. Alire, Intramolecular energy transfer in rare earth chelates. Role of the triplet state, J. Chem. Phys. 34 (1961) 743–748.
- [64] M.P. Tsvirko, S.B. Meshkova, V.Y. Venchikov, Z.M. Topilova, D.V. Bol'shoi, Determination of contributions of various molecular groups to nonradiative deactivation of electronic excitation energy in beta-diketonate complexes of ytterbium(III), Opt Spectrosc. 90 (2001) 669–673.
- [65] A. de Bettencourt-Dias, Introduction to lanthanide ion luminescence, in: Luminescence of Lanthanide Ions in Coordination Compounds and Nanomaterials, John Wiley & Sons Ltd, Chichester, 2014, pp. 1–48.

- [66] N.S. Makarov, M. Drobizhev, A. Rebane, Two-photon absorption standards in the 550-1600 nm excitation wavelength range, Opt Express 16 (2008) 4029–4047.
- [67] S.V. Eliseeva, G. Auböck, F. van Mourik, A. Cannizzo, B. Song, E. Deiters, A.-S. Chauvin, M. Chergui, J.-C.G. Bünzli, Multiphoton-excited luminescent lanthanide bioprobes: two- and three-photon cross sections of dipicolinate derivatives and binuclear helicates, J. Phys. Chem. B 114 (2020) 2932–2937.
- [68] F. Caillé, C.S. Bonnet, F. Buron, S. Villette, L. Helm, S. Petoud, F. Suzenet, É. Tóth, Isoquinoline-based lanthanide complexes: bright NIR optical probes and efficient MRI agents, Inorg. Chem. 51 (2012) 2522–2532.
- [69] A. de Bettencourt-Dias, P.S. Barber, S. Viswanathan, D.T. de Lill, A. Rollett, G. Ling, S. Altun, Para-derivatized pybox ligands as sensitizers in highly luminescent Ln(III) complexes, Inorg. Chem. 49 (2010) 8848–8861.
- [70] A. D'Aléo, G. Pompidor, B. Elena, J. Vicat, P.L. Baldeck, L. Toupet, R. Kahn, C. Andraud, O. Maury, Two-photon microscopy and spectroscopy of lanthanide bio-probes, ChemPhysChem: Eur.J. Chem. Phys. Phys. Chem. 8 (2007) 2125–2132.
- [71] E.R.H. Walter, J.A. Gareth Williams, D. Parker, Solvent polarity and oxygen sensitivity, rather than viscosity, determine lifetimes of biaryl-sensitized terbium luminescence, Chem. Commun. 53 (2017) 13344–13347.
- [72] I. Kutsche, G. Gildehaus, D. Schuller, A. Schumpe, Oxygen solubilities in aqueous alcohol solutions, J. Chem. Eng. Data 29 (1984) 286–287.
- [73] T. Sato, Y. Hamada, M. Sumikawa, S. Araki, H. Yamamoto, Solubility of oxygen in organic solvents and calculation of the hansen solubility parameters of oxygen, Ind. Eng. Chem. Res. 53 (2014) 19331–19337.
- [74] A.T. Bui, A. Grichine, A. Duperray, P. Lidon, F. Riobé, C. Andraud, O. Maury, Terbium(III) luminescent complexes as millisecond-scale viscosity probes for lifetime imaging, J. Am. Chem. Soc. 139 (2017) 7693–7696.
- [75] C. Andraud, O. Maury, Lanthanide complexes for nonlinear optics: from fundamental aspects to applications, Eur. J. Inorg. Chem. (2009) 4357–4371.